ELEMENTA
Science of the Anthropocene

Quantifying mercury isotope dynamics in captive Pacific bluefin tuna (*Thunnus orientalis*)

Sae Yun Kwon[1,2]* • Joel D. Blum[1] • Daniel J. Madigan[3] • Barbara A. Block[4] • Brian N. Popp[5]

[1]Earth and Environmental Sciences, University of Michigan, Ann Arbor, Michigan, United States
[2]Institute for Data, Systems, and Society, Massachusetts Institute of Technology, Cambridge, Massachusetts, United States
[3]Harvard University Center for the Environment, Harvard University, Cambridge, Massachusetts, United States
[4]Tuna Research and Conservation Center, Hopkins Marine Station of Stanford University, Pacific Grove, California, United States
[5]Department of Geology and Geophysics, University of Hawaii, Honolulu, Hawaii, United States

*saeyunk@umich.edu

Abstract

Analyses of mercury (Hg) isotope ratios in fish tissues are used increasingly to infer sources and biogeochemical processes of Hg in natural aquatic ecosystems. Controlled experiments that can couple internal Hg isotope behavior with traditional isotope tracers ($\delta^{13}C$, $\delta^{15}N$) can improve the applicability of Hg isotopes as natural ecological tracers. In this study, we investigated changes in Hg isotope ratios ($\delta^{202}Hg$, $\Delta^{199}Hg$) during bioaccumulation of natural diets in the pelagic Pacific bluefin tuna (*Thunnus orientalis*; PBFT). Juvenile PBFT were fed a mixture of natural prey and a dietary supplement (60% *Loligo opalescens*, 31% *Sardinops sagax*, 9% gel supplement) in captivity for 2914 days, and white muscle tissues were analyzed for Hg isotope ratios and compared to time in captivity and internal turnover of $\delta^{13}C$ and $\delta^{15}N$. PBFT muscle tissues equilibrated to Hg isotope ratios of the dietary mixture within ~700 days, after which we observed a cessation in further shifts in $\Delta^{199}Hg$, and small but significant negative $\delta^{202}Hg$ shifts from the dietary mixture. The internal behavior of $\Delta^{199}Hg$ is consistent with previous fish studies, which showed an absence of $\Delta^{199}Hg$ fractionation during Hg bioaccumulation. The negative $\delta^{202}Hg$ shifts can be attributed to either preferential excretion of Hg with higher $\delta^{202}Hg$ values or individual variability in captive PBFT feeding preferences and/or consumption rates. The overall internal behavior of Hg isotopes is similar to that described for $\delta^{13}C$ and $\delta^{15}N$, though observed Hg turnover was slower compared to carbon and nitrogen. This improved understanding of internal dynamics of Hg isotopes in relation to $\delta^{13}C$ and $\delta^{15}N$ enhances the applicability of Hg isotope ratios in fish tissues for tracing Hg sources in natural ecosystems.

Introduction

Mercury (Hg) in marine ecosystems is a significant public health concern due to the transformation of atmospherically transported inorganic Hg (IHg) to monomethylmercury (MMHg) in the oceans. MMHg is the toxic and bioaccumulative form of Hg that can bioaccumulate and biomagnify to elevated levels in high trophic level fish (Mergler et al., 2007). In the open ocean, MMHg is believed to form via biological processes at oxic/anoxic interfaces at intermediate depths or within water column oxygen minimum zones (Sunderland et al., 2009; Blum et al., 2013). MMHg may also be introduced externally from deep hydrothermal vents (Kraepiel et al., 2003; Lamborg et al., 2006) and via bioadvection from coastal shelves (i.e., via migratory fish; Lawson and Mason, 1998; Hammerschmidt and Fitzgerald, 2006), but these inputs are minor compared to in situ methylation (Cossa et al., 1996, 2009). A consequence of MMHg bioaccumulation in

marine food webs is that over 90% of the total Hg (THg) in commercial fisheries products is present as MMHg (Sunderland, 2007).

Studies of sources and fate of MMHg in marine ecosystems have been extensive (e.g., Kraepiel et al., 2003; Sunderland et al., 2009; Mason et al., 2012; Coleman et al., 2015; Drevnick et al., 2015). These studies have collectively demonstrated that the ability to link MMHg source to receptor is challenged by the presence of multiple sources, dynamic biogeochemical processing of MMHg, and potential ecological changes affecting MMHg sources. For instance, recent studies have measured long-term changes in Hg levels in Pacific yellowfin tuna (*Thunnus albacares*) in order to distinguish the relative importance of anthropogenic versus natural Hg sources to open ocean waters, and have reported contrasting results (Kraepiel et al., 2003; Drevnick et al., 2015). Other studies have quantified Hg levels in diverse marine organisms and suggested that the bioaccumulative sources of MMHg may be related to feeding depths (Choy et al., 2009) and life history characteristics (i.e., trophic positions, age, size) of marine organisms (Hammerschmidt and Fitzgerald, 2006; Szczebak and Taylor, 2011). In addition, it is predicted that increasing ecological changes resulting from climate change (i.e., ocean circulation patterns, increased productivity, expansion of oxygen minimum zones) (Olson et al., 2014; Pethybridge et al., 2015) will likely affect future sources and biogeochemical cycling of MMHg in marine ecosystems (Krabbenhoft and Sunderland, 2013). Understanding of the sources and fate of MMHg in marine ecosystems, by effectively linking MMHg sources to receptors, will be further elucidated with development and refinement of new techniques.

One such technique is the measurements of Hg stable isotopes, which has recently improved the understanding of the sources and biogeochemical processes governing MMHg in natural ecosystems. Hg has seven stable isotopes that exist naturally in the environment (^{196}Hg = 0.155%, ^{198}Hg = 10.04%, ^{199}Hg = 16.94%, ^{200}Hg = 23.14%, ^{201}Hg = 13.17%, ^{202}Hg = 29.73%, ^{204}Hg = 6.83%) (Blum and Bergquist, 2007). Hg isotopes can undergo fractionation by two types of pathways that impart distinct Hg isotopic compositions on natural environmental samples. Mass-dependent fractionation (MDF), reported as $\delta^{202}Hg$ values in units of permil (‰ Blum and Bergquist, 2007), occurs via various environmentally relevant processes such as microbial methylation (Rodriguez-Gonzalez et al., 2009; Perrot et al., 2015), demethylation (Kritee et al., 2009), thiol-ligand exchange (Wiederhold et al., 2010), sorption (Jiskra et al., 2012), diffusion (Koster van Groos et al., 2014), precipitation of metacinnabar and montroydite (Smith et al., 2015), and photochemical degradation (Bergquist and Blum, 2007; Zheng and Hintelmann, 2009). In contrast to MDF, significant mass-independent fractionation (MIF), reported as $\Delta^{199}Hg$ values (‰; Blum and Bergquist, 2007), is thought to occur predominantly during photochemical reduction and degradation of IHg and MMHg (Bergquist and Blum, 2007; Zheng and Hintelmann, 2009). By combining MDF and MIF, previous studies have identified sources and gained insight into complex biogeochemical processes governing MMHg in many natural ecosystems (Gantner et al., 2009; Senn et al., 2010; Gehrke et al., 2011; Point et al., 2011; Day et al., 2012; Perrot et al., 2012; Tsui et al., 2012, 2013, 2014; Blum et al., 2013; Demers et al., 2007; Sherman and Blum, 2013; Kwon et al., 2014, 2015).

Particularly in aquatic ecosystems, the analysis of Hg isotope ratios in fish tissues has become a useful tool for monitoring complex biological processes such as bioaccumulation and trophic transfer, and consequently for inferring bioaccumulative sources of MMHg (Gantner et al., 2009; Senn et al., 2010; Gehrke et al., 2011; Point et al., 2011; Perrot et al., 2012; Tsui et al., 2012, 2013, 2014; Blum et al., 2013; Sherman and Blum, 2013; Kwon et al., 2014, 2015). For instance, fish feeding experiments documented the absence of $\delta^{202}Hg$ and $\Delta^{199}Hg$ fractionation during bioaccumulation and trophic transfer of both IHg and MMHg to juvenile freshwater (i.e., yellow perch) and marine fish (i.e., amberjack) (Kwon et al., 2012, 2013). This absence indicated that the isotopic composition in fish reflects that of fish prey, which in turn reflects environmental sources of Hg accumulated from the base of the food web and retained in fish tissues. By coupling traditional isotope tracers (i.e., $\delta^{13}C$ and $\delta^{15}N$), previous studies also characterized Hg isotope ratios in a diverse range of species of aquatic organisms in order to distinguish between bioaccumulative sources of MMHg in various marine compartments (i.e., coastal versus pelagic, sediment versus water-column feeder) (Senn et al., 2010; Perrot et al., 2012). The applicability of Hg isotope ratios in fish tissues as a natural ecological tracer can be further expanded with additional experiments that quantify the retrospective time frames represented by measured fish Hg isotope ratios, assess the influence(s) of metabolic processes on the fractionation of Hg isotopes, and couple internal behaviors of Hg isotopes with traditional isotope tracers. Lack of long-term controlled experiments limits the interpretation of Hg isotope ratios in fish tissues, particularly in the face of fluctuating environmental and ecological conditions affecting future sources of MMHg in marine ecosystems (Krabbenhoft and Sunderland, 2013).

We investigated long-term changes in Hg isotope ratios ($\delta^{202}Hg$ and $\Delta^{199}Hg$) during bioaccumulation of natural diets in the Pacific bluefin tuna (*Thunnus orientalis*), which is a relevant study subject given its increasing commercial value for human consumption (Sunderland, 2007) and its ecological characteristics. Pacific bluefin tuna are an important component of the pelagic ecosystem because they are long-lived (> 25 years) (Shimose et al., 2009), and widely distributed (Block et al., 2001), allowing them to integrate spatially and temporally variable MMHg sources from the water column. In this study, juvenile Pacific bluefin tuna were fed natural diets (i.e., mainly sardine and squid) in captivity for a total of 2914 days, and either sacrificed

or collected upon natural mortality at different time periods. White muscle tissues of Pacific bluefin tuna were analyzed for Hg isotope ratios, and these ratios were related to time in captivity. The Hg isotopic compositions of Pacific bluefin tuna muscle tissues were also characterized in relation to the internal turnover of $\delta^{13}C$ and $\delta^{15}N$ values in bulk muscle tissues and in proteinaceous amino acids, which are published elsewhere (Madigan et al., 2012; Bradley et al. 2014). This study is the first attempt to understand long-term changes in Hg isotope ratios in large, pelagic, regionally endothermic fish and may ultimately improve the application of Hg isotope ratios in fish tissues as a tracer for sources of MMHg in marine ecosystems.

Materials & methods

1.1 Captive husbandry

Details of the sampling location, tuna holding, and tissue sampling were previously published in Madigan et al. (2012) and Estess et al. (2014). Briefly, juvenile (1.1–1.5 year old Pacific bluefin tuna (*Thunnus orientalis*; PBFT hereafter) were collected using hook and line from the California Current waters, USA, and northern Baja California, Mexico. The curved fork length (or the linear distance from the tip of the upper jaw of the fish to the tip of the tail) of individuals ranged from 63–70 cm. The PBFT were transported and raised at the Tuna Research and Conservation Center (TRCC) at Hopkins Marine Station, Stanford University, for the first 700 days prior to being transported to the Monterey Bay Aquarium (MBA). At the MBA, the remaining PBFT were raised up to 2214 days (a total of 2914 days) prior to reaching natural mortality. At both study locations (TRCC and MBA), the PBFT were kept in tanks maintained by a flow-through system and were held over the course of the study at a relatively constant temperature of ~20°C.

During the entire holding period, the PBFT were fed with a mixture of a natural diet of 60% squid (*Loligo opalescens*) and 31% sardine (*Sardinops sagax*), plus 9% dietary supplement (gel). Squid and sardine were purchased commercially (origin from Monterey Bay, California, USA) during each season for two consecutive years (2010–2011). The gel, composed mainly of by-catch products, gelatin, algae, and vitamins, was purchased commercially from Mazuri (Low Fat Aquatic Gel Diet). PBFT were fed the dietary mixture three times a week, and the mass of the dietary mixtures was adjusted proportionally to total estimated body mass of PBFT (with a ratio of squid:sardine:gel:PBFT of 0.04:0.02:0.005:1). Individual PBFT were either sacrificed for other experiments or collected upon natural mortality at different time periods and dissected for white muscle tissues. Subsamples of PBFT white muscle tissues and dietary mixtures were kept frozen at −20°C prior to analysis of $\delta^{13}C$, $\delta^{15}N$, THg concentration, and THg isotope ratios. THg concentrations are reported in dry weight.

1.2 $\delta^{13}C$, $\delta^{15}N$ and THg and MMHg concentration analyses

The PBFT and the dietary mixtures were analyzed for $\delta^{13}C$ and $\delta^{15}N$ values at the Stanford Stable Isotope Biogeochemistry Laboratory and for individual amino acids at the Stable Isotope Biogeochemistry Laboratory, University of Hawaii. Details of the stable isotope methods and results were previously published in Madigan et al. (2012) and Bradley et al. (2014). Briefly, samples were frozen at −80°C, lyophilized for 72 hours, and ground to a fine powder. The $\delta^{13}C$ and $\delta^{15}N$ values in bulk muscle tissues were measured using a Thermo Finnigan Delta-Plus IRMS coupled to a Carlo Erba NA1500 Series 2 elemental analyzer via a Thermo Finnigan Conflo II interface. Isotope values are expressed in the standard $\delta^{13}C$ and $\delta^{15}N$ notation (‰) relative to international standards (PeeDee belemnite and atmospheric N_2, respectively). Analytical precision was quantified using internationally calibrated standards; USGS 24, USGS 40, IAEA N1, and acetanilide interspersed every 8 samples. The analytical uncertainty of $\delta^{13}C$ and $\delta^{15}N$ was < 0.15‰. Individual amino acids were derived following established methods (Hannides et al., 2009) and measured using a Delta V Mass spectrometer interfaced to a Trace GC gas chromatograph through a GC-C III combustion furnace, reduction furnace, and liquid nitrogen cold trap via a GC-C III interface. Measured $\delta^{15}N$ values were normalized to the known N isotopic composition of internal references norleucine and aminoadipic acid co-injected with each sample. All samples were analyzed in triplicates and the standard deviation of $\delta^{15}N$ values ranged between 0.03‰ and 1.2‰.

Subsamples of the lyophilized and powdered PBFT white muscle tissue and dietary mixtures were measured for THg and MMHg concentration at Stony Brook University and at Harvard University, respectively. THg concentration was measured using a Milestone DMA-80 Direct Mercury Analyzer (detection limit: 0.005 ng). The DMA-80 was calibrated with a 1.0 ug g^{-1} Hg standard solution (VHG Labs, Inc.), and the standard solution and certified reference material NRCC DORM-4 (fish protein) were analyzed with samples to validate quality assurance. Recoveries of DORM-4 were 0.401 ± 0.027 ug g^{-1} (certified value 0.410 ± 0.055 ug g^{-1}). Standard solution and DORM-4 calibration checks were performed every ten samples to monitor DMA-80 stability. To evaluate reproducibility, samples were run in duplicate for every 10 samples, and overall variation of duplicates was < 3%. Six of the twelve PBFT samples (11, 591, 723, 1189, 1947, and 2289 days in captivity) and samples of sardine and squid food sources were analyzed for MMHg concentration.

Lyophilized and powdered samples were digested in 5 M HNO_3 at 60°C overnight and neutralized with 8 M KOH. MMHg concentration was measured using a Tekran Model 2700 Automated MethylMercury Analysis System (detection limit: 0.004 ng) calibrated with a 1000 ug g^{-1} MMHg standard solution (Alfa Aesar). Recoveries of standard solutions (diluted to two different concentrations) and certified reference material NRCC DORM-4 and NRCC TORT-3 (lobster hepatopancreas) were $102 \pm 14\%$ (n = 3), $99 \pm 14\%$ (n = 3), 94% (n = 1), and 86% (n = 1), respectively. To evaluate reproducibility, samples were run in triplicates, and overall variation of triplicates of the samples was $\pm 5\%$. All MMHg values are presented as the fraction of THg present as MMHg (%).

1.3 Hg stable isotope analyses

PBFT muscle tissues and the dietary mixtures were measured for Hg isotope ratios at the University of Michigan. Freeze-dried samples were homogenized into a fine powder, weighed, and loaded into ceramic boats with Na_2CO_3 and Al_2O_3 powders. The samples were combusted in an offline two-stage combustion furnace to release Hg^0 from the samples. Released Hg^0 was captured into a trap solution containing 1% $KMnO_4$ in 10% trace metal grade H_2SO_4. To remove combustion residues from the samples, the trap solutions containing sample Hg were neutralized with NH_2OH, reduced back to Hg^0 with $SnCl_2$, and purged into a new trap solution. The recoveries of the combustion and transfer steps were monitored by measuring THg in the trap solutions containing samples, the standard reference materials ERM CE 464 (tuna tissue; n = 3), and NIST 1947 (Lake Michigan fish tissue; n = 2). The blanks were also monitored by trapping and measuring THg released from Na_2CO_3 and Al_2O_3 powders and ceramic boats alone (without samples). The THg in the trap solutions was determined by cold vapor atomic absorption spectroscopy (CV-AAS; Nippon MA-2000). The procedural blanks had an average THg of 0.14 ± 0.04 ng (n = 3). The recoveries of the combustion and transfer steps of all the samples and standard reference materials ranged between 93 and 105%, and 90 and 102%, respectively.

Mercury isotope ratios were measured using a Nu Instruments multi-collector inductively coupled plasma mass spectrometer (MC-ICP-MS). Sample Hg captured in trap solutions was introduced to the MC-ICP-MS by continuously reducing Hg^{2+} with 2% $SnCl_2$, and separating Hg^0 using a frosted glass tip phase separator. Instrumental mass bias was corrected using an internal Tl standard (NIST SRM 997) and by bracketing each sample with NIST SRM 3133 prepared to match the matrix composition and THg concentration of the samples. MDF is reported as $\delta^{202}Hg$ (in units of ‰) referenced to NIST SRM 3133 (Blum and Bergquist, 2007):

$$\delta^{202}Hg = \{[(^{202}Hg / ^{198}Hg)_{sample} / (^{202}Hg / ^{198}Hg)_{NIST3133}] - 1\}*1000$$

MIF represents the difference between the measured $\delta^{xxx}Hg$ value and the value predicted based on MDF and the $\delta^{202}Hg$ value. MIF is reported as $\Delta^{199}Hg$, and $\Delta^{201}Hg$ (in units of ‰) (Blum and Bergquist, 2007). The calculation is based on an approximation valid for $\delta < 10$‰:

$$\Delta^{199}Hg = \delta^{199}Hg - (\delta^{202}Hg * 0.252)$$

$$\Delta^{201}Hg = \delta^{201}Hg - (\delta^{202}Hg * 0.752)$$

Analytical uncertainty at 2 SD is estimated based on either replicate analyses of our standard solution (UM-Almadén) or replicate analyses of standard reference materials (ERM CE 464 and NIST 1947). We used ERM CE 464 to report analytical uncertainty since it had the largest uncertainty. UM-Almadén (n = 54) had mean values $\pm$ 2 SD of $\delta^{202}Hg = -0.57 \pm 0.12$‰, and $\Delta^{199}Hg = -0.03 \pm 0.10$‰. Standard reference material ERM CE 464 (n = 3) had mean values of $\delta^{202}Hg = 0.71 \pm 0.12$‰ and $\Delta^{199}Hg = 2.42 \pm 0.06$‰, and NIST 1947 (n = 2) had mean values of $\delta^{202}Hg = 1.27 \pm 0.02$‰ and $\Delta^{199}Hg = 5.51 \pm 0.06$‰.

Results

1.1 THg concentrations & Hg isotopic compositions of the dietary mixture

Mean THg concentrations of the gel, squid, and sardine were 88.4 ± 1.2 ng g^{-1} (n = 2, 1 SD), 76.5 ± 12.1 ng g^{-1} (n = 3, 1 SD), and 151 ± 42.2 ng g^{-1} (n = 3, 1 SD), respectively (Table 1). The % MMHg values (the fraction of THg present as MMHg) of the squid and sardine were $99.0 \pm 7.0\%$ (n = 3, 1 SD), and $76.2 \pm 4.0\%$ (n = 3, 1 SD), respectively. These values confirm previous results from the literature that most Hg in these food sources is in the form of MMHg (Caurant et al., 1996; Joiris et al., 1999; Das et al., 2000). Mean $\delta^{202}Hg$ values of the gel, squid, and sardine were 0.05 ± 0.05‰, 0.11 ± 0.09‰, and 0.71 ± 0.13‰, respectively, and mean $\Delta^{199}Hg$ values were 0.85 ± 0.01‰, 1.73 ± 0.15‰, and 1.75 ± 0.10‰, respectively (Table 1). The Hg isotopic compositions of the squid and sardine are within the range of fish values reported by Senn et al. (2010), who analyzed fish from the coastal and transition regions of the Gulf of Mexico, USA. The relatively high THg concentrations and the significant positive $\Delta^{199}Hg$ values observed in the gel most likely reflect

Table 1. Total mercury (THg) concentration (ng g⁻¹), Hg isotope values, and mass proportion (%) used to prepare the dietary mixture composed of gel, sardine, and squid

Diets	Hg (ng g^{-1})	δ^{202}Hg (‰)	δ^{199}Hg (‰)	Δ^{201}Hg (‰)	Mass proportion of diet (%)
Gel 1	87.6	0.07	0.85	0.70	9
Gel 2	89.3	0.02	0.84	0.69	
Average	88.4	0.05	0.85	0.70	
1 SD	1.21	0.04	0.01	0.01	
Squid 1	89.2	0.01	1.56	1.30	60
Squid 2	65.1	0.16	1.83	1.50	
Squid 3	75.2	0.17	1.80	1.50	
mean	76.5	0.11	1.73	1.43	
1 SD	12.1	0.09	0.15	0.12	
Sardine 1	155	0.66	1.84	1.55	31
Sardine 2	191	0.86	1.78	1.54	
Sardine 3	107	0.62	1.64	1.37	
mean	151	0.71	1.75	1.49	
1 SD	42.2	0.13	0.10	0.10	
Weighted mean[a]	101 [80.1–121]	0.39 [0.29–0.48]	1.67 [1.54–1.76]	1.39 [1.28–1.45]	
Weighted SD	20.5	0.10	0.12	0.10	

[a]Values in brackets represent the ranges of THg concentrations and Hg isotope values of the dietary mixture

doi: 10.12952/journal.elementa.000088.t001

by-catch products used during the manufacturing of the gel (see Materials and methods). High positive Δ^{199}Hg values were previously reported in commercial food pellets composed mainly of marine by-catch (Kwon et al., 2012). In that study, the high positive Δ^{199}Hg values were attributed to MMHg photochemical degradation prior to bioaccumulation into the marine food web and ultimately to fish. Using the mass proportion of each dietary component in the dietary mixture (9% gel, 60% squid, 31% sardine), we calculated the weighted mean of THg concentration and Hg isotopic composition of the dietary mixture fed to PFBT throughout the holding period. Weighted mean THg concentration of the dietary mixture was 101 ng g⁻¹ and the weighted mean δ^{202}Hg and Δ^{199}Hg values were 0.39‰ and 1.67‰, respectively (Table 1).

1.2 THg concentrations of PBFT

THg concentrations in PBFT white muscle tissue ranged from 0.84 to 2.58 ug g⁻¹ (Table 2). The average % MMHg value of PBFT white muscle tissues was 91.8 ± 12% (n= 6, 1 SD). THg concentrations of PBFT muscle tissue became increasingly variable and displayed an overall decreasing trend from 2.58 ug g⁻¹ to 1.51 ug g⁻¹ with increasing time in captivity (Figure 1). The average muscle tissue THg at the longest time periods (after equilibration) is ~12 times higher than the THg of the dietary mixture, which illustrates the bioaccumulation factor (THg concentration of PBFT white muscle tissue divided by the weight mean THg concentration of the dietary mixture). The small decreasing trend in THg concentration with time in captivity is consistent with previous studies, which reported THg concentrations in captive and farmed PBFT (Nakao et al., 2007; Lares et al., 2012; Coleman et al., 2015). These studies attributed the reduction in THg concentration to internal biodilution due to growth. In this study, the ratio of the mass of the dietary mixture to the mass of PBFT was kept constant. Complete details of PBFT growth in captivity is published in Madigan et al. (2012). Among the individuals analyzed for Hg isotope ratios (this study), we found that the body mass of the PBFT increased by a factor of 47 (4.69 kg to 220 kg) during the experimental period (Table 2). Assuming that the PBFT consumed all the dietary mixture provided, we calculated the rate at which THg associated with the dietary mixture was taken up by PFBT ([THg] of the dietary mixture (mg g⁻¹) * mass of the dietary mixture at either initial or final time (g) / 3 days = rate of THg uptake from

Table 2. Total mercury (THg) concentration (ug g⁻¹), % MMHg, stable carbon and nitrogen isotope values, and Hg isotope values of white muscle tissues of PBFT for given body length, mass and time in captivity[a]

Time in captivity (days)	Curved fork length[b] (cm)	Mass (kg)	Hg (ug g⁻¹)	% MMHg	δ^{202}Hg (‰)	δ^{199}Hg (‰)	Δ^{201}Hg (‰)	δ^{13}C (‰)[c,d]	δ^{15}N (‰)[d]
11	67.5	4.69	2.58	110	0.55	1.84	1.55	–16.9	12.9
58	70.0	6.05	1.70	N/A	0.66	2.20	1.80	–17.8	12.9
95	82.0	8.77	1.90	N/A	0.48	1.97	1.68	–16.8	12.9
219	75.4	8.00	2.10	N/A	0.64	2.18	1.75	–17.1	14.3
416	85.2	12.2	1.59	N/A	0.54	1.95	1.59	–16.2	15.2
481	97.0	17.9	1.68	N/A	0.29	1.77	1.46	–15.4	15.2
591	91.0	13.3	1.14	81	0.44	1.70	1.37	–16.5	15.3
723	92.3	14.4	1.45	86	0.29	1.69	1.45	–16.0	15.4
1189	144	56.3	1.02	94	0.20	1.61	1.34	–15.0	15.7
1947	156	84.0	0.84	78	0.25	1.71	1.39	–15.5	15.7
2289	188	134	1.96	102	0.22	1.62	1.30	–15.5	16.1
2914	211	220	1.51	N/A	0.19	1.64	1.40	–15.9	16.1

[a]N/A = not analyzed
[b]Length of line from tip of the upper jaw to the tip of the tail.
[c]Arithmetically lipid-corrected values or those corrected mathematically by normalizing δ^{13}C values based on bulk C:N values (by mass). Correction is used to eliminate δ^{13}C bias caused by the variability in tissue lipid content
[d]Reported in Madigan et al. (2012)
doi: 10.12952/journal.elementa.000088.t002

the dietary mixture (mg day⁻¹)). We estimate that the uptake rate of THg increased proportionally with body mass from 10.2 mg THg day⁻¹ to 478 mg THg day⁻¹. We attribute the small reduction in THg at the two longest time periods (Figure 1) and the general variability in THg concentration of the PBFT to variability in growth rates, consumption rates, and/or feeding preferences of the individual PFBT. Alternatively, it is possible that the excretion of MMHg during tissue turnover may cause reduction in PBFT THg concentration (see discussion below).

1.3 Hg isotopic compositions of PBFT

The δ^{202}Hg and Δ^{199}Hg values of the PBFT at day 11 (the first time step available) were 0.55‰ and 1.84‰, respectively (Table 2). The Hg isotopic composition of PBFT at this time period is consistent with Blum et al. (2013), who reported values for marine fish, including yellowfin tuna, collected at intermediate depths (200–400 m) from offshore regions of the Pacific Ocean. The δ^{202}Hg and Δ^{199}Hg values of PBFT muscle tissue shifted towards the isotopic composition of the dietary mixture with increasing time in captivity (Figure 2). At time ~700 days, δ^{202}Hg and Δ^{199}Hg values of PBFT nearly equaled the isotopic composition of the dietary mixture (Figure 2). After 700 days, we observed a cessation in further shifts in Δ^{199}Hg, and small but significant negative shifts in δ^{202}Hg (–0.19‰) in PBFT compared to values of the dietary mixture.

In order to better understand the internal changes in Hg isotopes in the PBFT, we applied the exponential fit model that has been used to describe δ^{15}N and Δ^{13}C turnover in a wide range of species of fish, mammals,

$y = 3.23e^{-0.12}$
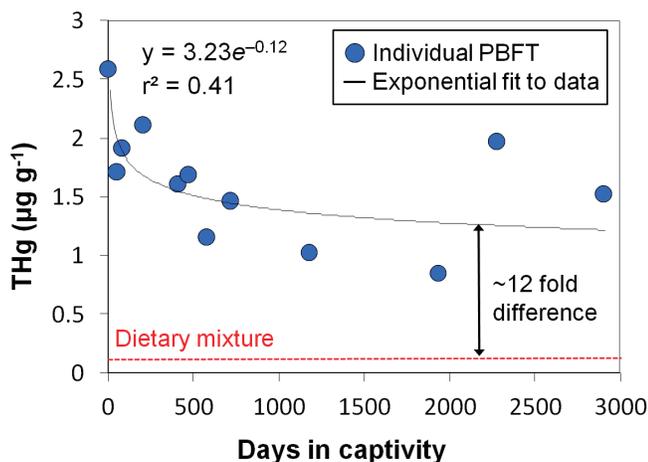$r^2 = 0.41$

● Individual PBFT
— Exponential fit to data

~12 fold difference

Dietary mixture

Figure 1

THg concentration (µg g⁻¹) of PBFT white muscle tissue with respect to time in captivity.

Black line shows exponential fit to PBFT data. Red dotted line represents the weighted mean THg concentration of the dietary mixture.

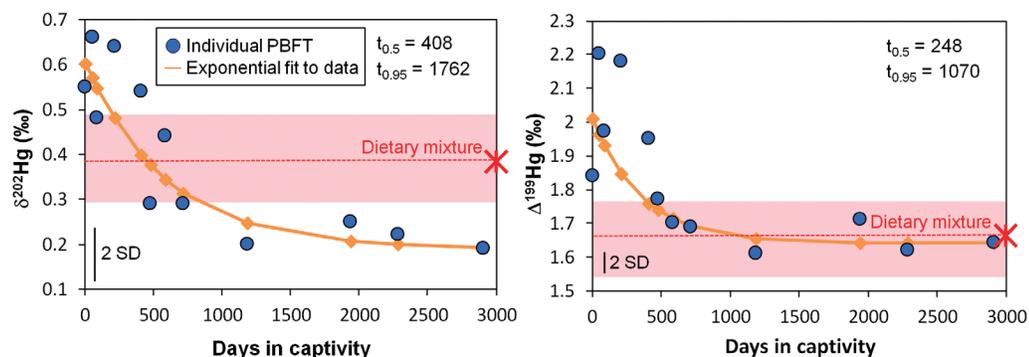doi: 10.12952/journal.elementa.000088.f001

and birds (Tieszen et al., 1983; MacAvoy et al., 2006; Madigan et al., 2012) (Figure 2). The equation for the exponential fit model describing isotopic turnover (Tieszen et al., 1983) is:

$$^{XXX}Hgt = ae^{-\lambda t} + c$$

where ^{XXX}Hgt represents either δ^{202}Hg or Δ^{199}Hg values at time t, a represents the difference between initial and final steady-state isotope ratio, c represents the final steady-state isotope ratio, and λ represents the first-order rate constant (days^{-1}). Note that we were unable to obtain PBFT muscle tissues at point of capture (at day 0), thus the initial δ^{202}Hg and Δ^{199}Hg values are represented by the mean Hg isotope values of PBFT at the first two time periods in captivity (11 and 58 days). These two initial Hg isotope values of PBFT (11 and 58 days) prior to long term holding and feeding were averaged to account for inter-individual variability at the start of the experiment. We found that the internal behavior of Hg isotopes, representing the assimilation of the dietary mixture, was adequately described by the exponential fit model (Figure 2).

In addition, we applied the reaction progress variable model to evaluate whether a single-compartment model with first-order kinetics or a multi-compartment model best describes the internal changes in Hg isotopes in PBFT. The equation for the reaction progress variable (Cerling et al., 2007) is:

$$(1-F) = {}^{XXX}Hgt - c\ /\ {}^{XXX}Hgi - c$$

where $(1-F)$ represents the fractional approach to steady-state ($F = 0$ represents the beginning of the exchange reaction, $F = 1$ at steady-state), ^{XXX}Hgt represents either δ^{202}Hg or Δ^{199}Hg values at time t, ^{XXX}Hgi represents initial δ^{202}Hg or Δ^{199}Hg values, and c represents the final steady-state isotope ratio. We observed a significant linear fit between $\ln(1-F)$ and time in captivity for both δ^{202}Hg ($r^2 = 0.55$, $p < 0.05$), and Δ^{199}Hg ($r^2 = 0.65$, $p < 0.05$). We also did not observe significant changes in slope on a plot of $\ln(1-F)$ with respect to time in captivity. These findings indicate that a single compartment model adequately describes the internal behavior of Hg isotopes (Cerling et al., 2007).

Using the exponential fit model, we calculated the half-lives and the steady-states of δ^{202}Hg and Δ^{199}Hg using the equation (in units of days; Tieszen et al., 1983; Buchheister and Latour, 2010):

$$t_x = \ln(2)\ /\ \lambda$$

where x represents either 0.5 (half-life) or 0.95 (steady-state), and λ represents the first-order rate constant (days^{-1}). The half-lives of δ^{202}Hg and Δ^{199}Hg were 408 and 248 days, respectively, and times to steady-state of δ^{202}Hg and Δ^{199}Hg were 1762 and 1070 days, respectively (Table 3). These time frames are substantially longer compared to half-life and steady-state estimates for δ^{15}N ($t_{0.5} = 167$, $t_{0.95} = 721$) and similar to values for δ^{13}C ($t_{0.5} = 225$, $t_{0.95} = 1103$) in the bulk muscle tissues of the same captive PBFT (Madigan et al., 2012).

Table 3. Estimates of half-life of Hg, C and N isotopes and time to steady-state derived from the exponential fit model during internal turnover in PBFT white muscle tissues

Isotope (‰)	Half-life (days)	Steady-state (days)
δ^{202}Hg	408	1762
Δ^{199}Hg	248	1070
δ^{13}C	225[a,b]	1103[a,b]
δ^{15}N	167[b]	721[b]

[a]Arithmetically lipid-corrected values or those corrected mathematically by normalizing δ^{13}C values based on bulk C:N values (by mass). Correction is used to eliminate δ^{13}C bias caused by the variability in tissue lipid content
[b]Reported in Madigan et al. (2012)
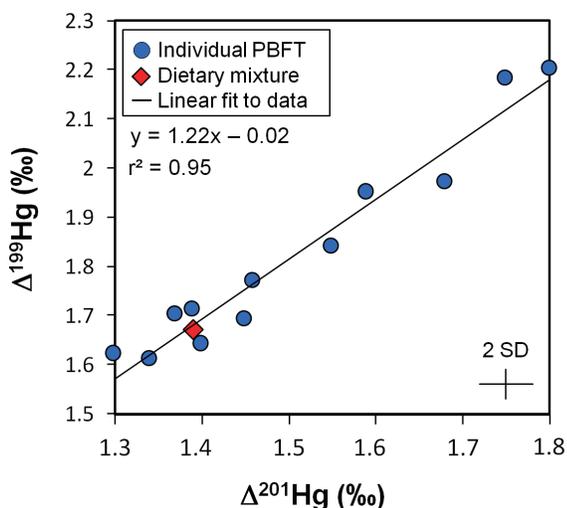doi: 10.12952/journal.elementa.000088.t003

The half-life and steady-state estimates of δ^{202}Hg and Δ^{199}Hg are within the ranges of those estimated for individual amino acids including glutamic acid ($t_{0.5}$ = 387, $t_{0.95}$ = 1671) and alanine ($t_{0.5}$ = 297, $t_{0.95}$ = 1283), respectively, in the same captive PBFT (Bradley et al., 2014).

1.4 Photochemical degradation of MMHg in the Pacific Ocean

In addition to understanding the internal behavior of Hg isotopes, we can use Hg isotope values of the PBFT to gain insight into photochemical reduction and degradation of IHg and MMHg in the Pacific Ocean. Previous fish feeding experiments have found an absence of Hg isotope fractionation during bioaccumulation and trophic transfer of both IHg and MMHg in freshwater and marine fish (Kwon et al., 2012, 2013). This absence indicated that Hg isotope ratios in fish tissues reflect Hg subjected to various biogeochemical processes (e.g., methylation, demethylation, photochemical reduction) prior to bioaccumulation into the base of the food web. The slope of Δ^{199}Hg / Δ^{201}Hg has been used to distinguish between photochemical reduction and degradation of IHg (Δ^{199}Hg / Δ^{201}Hg = 1.00), and MMHg (Δ^{199}Hg / Δ^{201}Hg = 1.2–1.4) (Bergquist and Blum, 2007). Using a York regression (York, 1966), we estimated the slope of Δ^{199}Hg / Δ^{201}Hg by applying values measured in PBFT muscle tissue. We found a slope of 1.22 ± 0.09 (r^2 = 0.95, p < 0.05) in PBFT; Δ^{199}Hg and Δ^{201}Hg values of the dietary mixture were within the ranges of this estimated slope (Figure 3). This slope is consistent with the photochemical degradation of MMHg observed in many marine food webs (~1.2) (Senn et al., 2010; Gehrke et al., 2011; Laffont et al., 2011; Point et al., 2011; Day et al., 2012; Blum et al., 2013).

Discussion

The long-term holding of PBFT at the Tuna Research and Conservation Center provided the opportunity to examine internal dynamics of Hg isotopes upon bioaccumulation of the dietary mixture. The internal dynamics of Hg isotopes of PBFT were compared to the few fish for which similar studies exist. This study revealed a longer time of equilibration for δ^{202}Hg and Δ^{199}Hg between diet and muscle tissue in PBFT compared to juvenile yellow perch *(Perca falvescens)* and amberjack *(Seriola dumerili)* (Kwon et al., 2012, 2013). Previous studies exposed juvenile yellow perch to food pellets spiked with synthetic MMHg and observed rapid equilibration of the muscle and liver tissues to δ^{202}Hg and Δ^{199}Hg values of the food pellets (Kwon et al., 2012). Juvenile amberjack fed with yellowfin tuna (i.e., containing natural MMHg) also displayed rapid equilibration of various tissues (i.e., muscle, liver, kidney, brain, blood) to the dietary δ^{202}Hg and Δ^{199}Hg values within ~30 days of the feeding experiment (Kwon et al., 2013). In the present study, we found that muscle tissues of ~1 year old PBFT equilibrated to the δ^{202}Hg and Δ^{199}Hg values of the dietary mixture composed mainly of MMHg within ~700 days in captivity. After ~700 days, we observed a cessation in further shifts in Δ^{199}Hg, and small but significant negative shifts in δ^{202}Hg in the PBFT muscle tissues from the values of the dietary mixture. Below we compare the results from previous fish feeding experiments (Kwon et al., 2012, 2013) to the present study to assess internal dynamics of Hg isotopes in PBFT.

1.1 Internal turnover of Hg isotopes

We first discuss the equilibration of Hg isotope values of the PBFT muscle tissues to the values of the dietary mixture (first ~700 days in captivity). Equilibration of fish tissues to Hg isotope values of the diet is a product of simple mixing and/or internal turnover of Hg isotopes upon bioaccumulation. Previous fish feeding experiments, using a binary isotope mixing model, described relatively rapid shifts in Hg isotope values in fish tissues to values of dietary MMHg (Kwon et al., 2012, 2013). However, there are important differences between the experimental design of these past studies and the present PBFT captivity conditions. In the study of juvenile yellow perch and amberjack, the fish were fed daily to satiation with unrealistically high concentrations of MMHg (ranging from 1.0 to 4.0 ug g^{-1}). Due to smaller initial size and higher relative growth rates, juvenile yellow perch and amberjack increased in body mass by 2–4-fold within 2–3 months of switching to high MMHg diets. In the present study, PBFT were fed with the dietary mixture that had ~26 times lower THg concentration than initial concentrations in the muscle tissues of PBFT. PBFT were also fed three times a week to provide energetic content similar to those in the wild, and demonstrated a consistent growth rate throughout the holding period (Madigan et al., 2012). The consistent growth rate suggests that while the juvenile yellow perch and amberjack were overwhelmed with MMHg by rapidly integrating experimental diets into body mass, the PBFT most likely had the opportunity to metabolize and replace previously accumulated MMHg during the long-term holding periods.

The overall internal behavior of Hg isotope ratios in the PBFT with respect to time in captivity was adequately described by the exponential fit model used to describe δ^{13}C and δ^{15}N turnover (Figure 2). Internal turnover is thought to be dependent on organism metabolism, defined as the sum of all internal processes governing synthesis and degradation of tissues (MacAvoy et al., 2006). Assimilation of new MMHg and remobilization and excretion of old MMHg during metabolic processes would cause internal turnover of Hg isotopes. MMHg accumulated via dietary uptake is most likely subjected to similar metabolic processes as C and N, which are the major components of tissues. MMHg is efficiently solubilized and absorbed in the gastrointestinal tract (Leaner and Mason, 2002). By forming a complex with thiol-ligands, MMHg is readily distributed to all tissues via the bloodstream before reaching the muscle tissue, which is the final storage organ for MMHg in fish (McCloskey et al., 1998; Oliveira Ribeiro et al., 1999). MMHg is also eliminated via the fecal route (Giblin and Massaro, 1973), which most likely occurs during the turnover of muscle tissue given the strong binding affinity of MMHg with thiol-ligands in muscle tissues.

PBFT have high metabolic rates, which may also be responsible for the internal turnover of Hg isotopes, as has been shown for δ^{13}C and δ^{15}N of bulk muscle tissues and in individual amino acids (Madigan et al., 2012; Bradley et al., 2014). Regionally endothermic fish such as PBFT have higher energy requirements owing to higher routine metabolic rates and specific dynamic action (i.e., energy expended after a feeding event) compared to ectothermic fish (Katz, 2002; Blank et al., 2007; Clark et al., 2013). Both laboratory and field studies have demonstrated that the rate of tissue turnover increases with metabolic rate, whereas growth only accounts for 10–20% of tissue turnover in most mammals and fish (MacAvoy et al., 2006; Weidel et al., 2011). By examining the turnover of δ^{13}C and δ^{15}N values in captive PBFT, Madigan et al. (2012) found that growth accounted for less turnover of δ^{13}C and δ^{15}N than did metabolism. Based on these results, we presume that internal turnover of Hg isotopes is most likely to occur in the PBFT with high metabolic activities compared to the juvenile amberjack and yellow perch (Kwon et al., 2012, 2013). Moreover, given that regionally endothermic fish have major blood vessels penetrating red and white muscle tissues for thermogenesis (Katz, 2002), it is possible that MMHg is subjected to more efficient bioaccumulation and remobilization in the warm muscle tissues of the PBFT.

1.2 Internal mass–dependent fractionation of Hg isotopes

In this section, we discuss the internal behavior of Hg isotopes upon equilibration of Hg isotope values of the PBFT to the values of the dietary mixture. After day ~700, we observed a cessation in further shifts in Δ^{199}Hg. The internal behavior is consistent with previous fish feeding studies, which showed an absence of Δ^{199}Hg fractionation during bioaccumulation and trophic transfer of IHg and MMHg (Kwon et al., 2012, 2013). The absence of Δ^{199}Hg fractionation in the PBFT confirms that Δ^{199}Hg is unaffected by metabolic processes, and thus predator Δ^{199}Hg values will reflect those of their prey. The δ^{202}Hg values displayed small but significant negative shifts in the PBFT muscle tissues from the values of the dietary mixture. We think that it is most likely that the negative δ^{202}Hg shift in the PBFT is due to internal MDF (discussed below). Alternatively, there was appreciable isotopic variability in diet items (sardine, squid, gel; Table 1), making it possible that our estimates of individual dietary δ^{202}Hg values differed by 0.1–0.2‰ from the long-term weighted mean of the dietary mixture (Table 1, Figure 2).

Multiple internal processes may be capable of causing fractionation of δ^{202}Hg. Juvenile amberjack exposed to a shrimp diet showed significant positive δ^{202}Hg shifts (+0.35‰) in various tissues compared to the values of the shrimp (Kwon et al., 2013). In that study, it was suggested that internal demethylation, which causes the MMHg remaining in an organism to display a higher δ^{202}Hg value compared to the product IHg (Kritee et al., 2009), and the preferential bioaccumulation of remaining MMHg, may provide an explanation for the

positive δ^{202}Hg shifts observed in the amberjack tissues. Internal demethylation has also been used to explain anomalously high positive δ^{202}Hg values observed in mammals, birds, and human hair (Laffont et al., 2011; Day et al., 2012; Perrot et al., 2012; Sherman et al., 2013; Kwon et al., 2014, 2015; Li et al., 2014). The negative δ^{202}Hg shift documented in the PBFT studied here (–0.19‰) suggests that internal demethylation is an unlikely explanation. Instead, this behavior could be caused by preferential excretion of MMHg with higher δ^{202}Hg values. Experimental studies have shown that Hg bound to thiol-ligands can have lower δ^{202}Hg values compared to the unbound Hg in solution (Wiederhold et al., 2010). Given that MMHg in muscle tissues is most often associated with thiol-ligands (Olson et al., 1978; Schultz and Newman, 1997), we presume that MMHg with higher δ^{202}Hg values is preferentially remobilized and excreted while MMHg bound to thiol-ligands with lower δ^{202}Hg values remains in the muscle tissues during internal turnover. In fact, we observed a decreasing trend in THg concentration in the PBFT with respect to time in captivity (Figure 1). Based on these observations, we propose that the excretion of MMHg during muscle tissue turnover is most likely responsible for the reduction in THg concentration and the negative δ^{202}Hg shifts observed in the PBFT. The fact that a significant amount of energy is devoted to excretion in PBFT (Estess et al., 2014) further supports the excretion of MMHg with higher δ^{202}Hg values as a plausible explanation for the negative shift in δ^{202}Hg.

An alternative explanation for the negative δ^{202}Hg shift is a small difference in the calculated weighted mean of δ^{202}Hg from the dietary mixture and the individual dietary δ^{202}Hg (squid, sardine, gel) presented to PBFT throughout the holding period. The sardine and squid collected at different times periods (refer to Materials and methods) had δ^{202}Hg ranges of 0.24‰ and 0.16‰ and δ^{199}Hg ranges of 0.20‰ and 0.27‰, respectively. The isotopic variability observed in sardine and squid is likely due to a combined effect of individual differences in life history (i.e., age, trophic position, size) (Whitlock et al., 2013) and temporal variation in environmental conditions. Based on this likelihood, it is possible that the individual PBFT with variable feeding preferences and/or consumption rates were exposed to dietary mixtures with slightly different δ^{202}Hg values throughout the long holding period. However, Δ^{199}Hg values were similarly variable yet displayed an absence of a shift between consumer and prey after equilibration (day ~700), suggesting that δ^{202}Hg fractionation is most likely caused by internal processes. In either case, we can say with confidence that the fractionation of δ^{202}Hg is either small (≤ 0.2‰) or nonexistent. The possibility of a slight fractionation should be considered when inferring predator feeding ecology using δ^{202}Hg.

1.3 Comparison with $\delta^{13}C$ and $\delta^{15}N$

In this section, we assess the internal behavior of Hg isotopes in relation to the turnover of δ^{13}C and δ^{15}N in PBFT. In Madigan et al. (2012), the same PBFT that were analyzed here for Hg isotopes were used to study C and N isotope turnover. C and N isotope values for the dietary mixture had higher δ^{13}C (–17.4‰) and δ^{15}N (13.9‰) values compared to the initial bulk muscle tissues of PBFT (δ^{13}C = –18.0‰, δ^{15}N = 11.8‰). The authors observed relatively rapid equilibration of δ^{13}C and δ^{15}N values of the PBFT muscle tissues to the values of the dietary mixture (within ~500 days). After the equilibration, the δ^{13}C values demonstrated a cessation in further shifts, which is consistent with previous studies that utilized δ^{13}C values to assess dietary resources in aquatic organisms (e.g., France, 1995; Fry, 2007; Jardine et al., 2012). The δ^{15}N values of the PBFT became ~2‰ higher compared to the dietary mixture. The half-lives and steady-states of δ^{202}Hg and Δ^{199}Hg were within the ranges of those estimated for individual amino acids including glutamic acid and alanine, respectively, in the same captive PBFT (Bradley et al., 2014).

The observation that the turnover rates of Hg isotopes are similar to individual amino acids but somewhat slower compared to N in bulk tissues suggests that Hg isotopes may interact with specific amino acids during the process of internal turnover. Previous studies have estimated binding affinities of MMHg to small amino acids including glutamic acid and alanine in both laboratory settings (Corbeil et al., 1986; Alex and Savoie, 1987) and by using biological media such as human erythrocytes (Rabenstein et al., 1982). These studies have demonstrated that, while MMHg demonstrates appreciable binding affinity with these amino acids (Corbeil et al., 1986; Alex and Savoie, 1987), the binding affinity is weak enough to lessen MMHg transport to various biological tissues when compared to thiol-ligands (Rabenstein et al., 1982). Other amino acids examined by Bradley et al. (2014) (i.e., glycine, lysine, serine, proline) displayed equally weak binding affinity with MMHg (Alex and Savoie, 1987). This weakness suggests that the similarity in the estimates of turnover rates between Hg isotopes and individual amino acids (Bradley et al., 2014) may be coincidental.

We attribute the slower turnover rates of Hg isotopes that we observed to slower bioaccumulation and elimination of MMHg from the muscle tissues compared to the bulk C and N. Our observations are consistent with previous studies in which internal half-lives of MMHg in a range of fish species were estimated at > 200 days (Jarvenpaa et al., 1970; Giblin and Massaro, 1973). These studies attributed the long internal half-life to the strong binding affinity of MMHg with thiol-ligands in the muscle tissues. Pharmacokinetic studies have also demonstrated that MMHg bioaccumulation and subsequent elimination in fish typically follows a biphasic trend, as a large fraction of MMHg first accumulates in visceral organs (i.e., intestine, liver) before being transported to the muscle tissue, which is the final storage organ for MMHg prior to excretion (Giblin

and Massaro, 1973; Oliveira Ribeiro et al., 1999). Conversely, it appears that the nutritional importance and the role of C and N in muscle exercise metabolism (Hemre et al, 2002) allow more efficient turnover of $\delta^{13}C$ and $\delta^{15}N$ in the internal system of PBFT.

It is important to note that the positive $\delta^{15}N$ shifts documented in PBFT contrast with the internal behavior of $\delta^{202}Hg$, which likely displayed small negative shifts from the values of the dietary mixture. In past studies, observed $\delta^{15}N$ values in predatory organisms were consistently higher by 2–3‰ than the dietary $\delta^{15}N$ values, which was attributed to the preferential excretion of ^{15}N versus ^{14}N during trophic transfer (Fry, 2007). The individual amino acids of glutamic acid and alanine in the same PBFT displayed even larger positive shifts of $\delta^{15}N$ (7.8‰ and 6.8‰) compared to the dietary values (Bradley et al., 2014). For Hg isotopes, we suggest that the strong binding affinity of MMHg with thiol-ligands in the muscle tissues, which causes preferential but slow excretion of MMHg with higher $\delta^{202}Hg$, is an important factor governing the internal behavior of Hg isotopes. Overall, the comparison of internal behavior of Hg isotopes with respect to $\delta^{13}C$ and $\delta^{15}N$ provides additional insight to the internal behavior of MMHg.

1.4 Applications

In summary, we observed internal turnover of Hg isotopes upon bioaccumulation of a dietary mixture in captive PBFT. After equilibration of Hg isotopes to the values of the dietary mixture, we observed what we believe to be the potential excretion of MMHg with higher $\delta^{202}Hg$ values. In contrast to $\delta^{202}Hg$, $\delta^{199}Hg$ displayed a cessation in further shifts from the values of the dietary mixture, confirming that internal processes do not cause fractionation of $\delta^{199}Hg$. The general internal behavior of Hg isotopes in PBFT is similar to $\delta^{13}C$ and $\delta^{15}N$, which operate on longer timescales compared to the bulk C and N. This behavior suggests that the elements C and N and the organic compound MMHg are subjected to similar metabolic processes during tissue turnover, but that MMHg turnover is slower in comparison to C and N.

The results of this long-term PBFT feeding experiment demonstrate the potential to enhance the applicability of Hg isotope ratios for tracing MMHg sources using fish tissues in natural ecosystems. Feeding experiments conducted in the past have determined tissue turnover rates from laboratory experiments by changing the diet of the organisms and measuring $\delta^{13}C$ and $\delta^{15}N$ in the tissues as they reach equilibrium with a new diet (e.g., MacAvoy et al., 2006). By establishing a relationship between Hg isotopes and $\delta^{13}C$ and $\delta^{15}N$ turnover our study demonstrates that Hg isotope ratios in fish tissues can be used to trace spatially and temporally variable MMHg sources. We suggest that the metabolism of organisms should be an important indicator for choosing which species to use when tracing MMHg sources in natural ecosystems. Rapid integration of MMHg isotopic compositions in juvenile fish (Kwon et al., 2012, 2013) indicates that Hg isotope ratios can be used in juvenile ectothermic fish to trace MMHg sources in regions affected by point source MMHg. In contrast, the slow integration and excretion of MMHg in PBFT suggest that it may be possible to use Hg isotope ratios in tuna to trace long-term changes in Hg isotope ratios, as tissues in these fish represent an integrated average of spatiotemporal variability in MMHg sources over some past time period.

Past studies have demonstrated that Hg isotope ratios in fish tissues can reflect changes in Hg sources and biogeochemical cycling, and are thus sensitive to environmental change. For instance, $\delta^{202}Hg$ values of fish tissues have been used to differentiate anthropogenic versus natural Hg sources (Gehrke et al., 2011; Kwon et al., 2014), while $\delta^{199}Hg$ values have been used to estimate the extent of photochemical degradation of IHg and MMHg in natural ecosystems (Senn et al., 2010; Gehrke et al., 2011; Point et al., 2011; Day et al., 2012; Blum et al., 2013; Sherman and Blum, 2013; Kwon et al., 2013, 2014). We found that $\delta^{199}Hg$ values of the PBFT shortly after capture (11 and 58 days in captivity) are consistent with marine fish collected from intermediate depths of the central Pacific Ocean (Blum et al., 2013). The initial PBFT collected for this study are recent migrants from the western Pacific Ocean (Madigan et al., 2014), where they feed at similar depths as those sampled in the central Pacific Ocean (Kitagawa et al., 2004; Blum et al., 2013) and reflect MMHg subjected to a similar extent of photochemical degradation within the water column. Similarly, $\delta^{13}C$ and $\delta^{15}N$ values of fish tissues have been used extensively to establish isoscapes in various marine ecosystems (Graham et al., 2010; Pethybridge et al., 2015). In particular, Pethybridge et al. (2015) measured $\delta^{13}C$ and $\delta^{15}N$ values in yellowfin tuna from the southwest Pacific Ocean and observed large-scale spatial variations, which were related to geography, productivity, and biological parameters such as size and age. By linking Hg isotopes with $\delta^{13}C$ and $\delta^{15}N$ of fish tissues, it may be possible to assess how environmental and ecological conditions are related to MMHg production and bioaccumulation in various ecosystem compartments.

It has been predicted that environmental and ecological changes introduced by climate change may affect future sources and biogeochemistry of MMHg in marine ecosystems (Krabbenhoft and Sunderland, 2013). By measuring long-term changes in $\delta^{13}C$ and $\delta^{15}N$ values in yellowfin tuna, Olson et al. (2014) found decadal dietary shifts caused by climate change in the eastern Pacific Ocean. Given that tuna demonstrate slow turnover of Hg isotopes, we may be able to link long-term changes in Hg isotope ratios with $\delta^{13}C$ and $\delta^{15}N$ to predict how future environmental and ecological changes will affect bioaccumulative sources of MMHg. Moreover, the fact that the exponential fit model adequately represents the internal behavior of Hg

isotopes suggests that this model can be used to estimate when these fish will reach steady-state with new MMHg sources. Time-integrative assessments of Hg isotope values in fish are important, as a number of studies have demonstrated that measuring Hg concentrations alone may be inadequate for differentiating the relative importance of natural versus anthropogenic sources of Hg (Kraepiel et al., 2003; Drevnick et al., 2015).

A number of limitations exist when applying our results to natural ecosystems. The small observed fractionation of δ^{202}Hg within PBFT suggests that we should be cautious when interpreting small shifts in δ^{202}Hg values in fish tissues to infer changes in MMHg sources in natural ecosystems. In addition, we emphasize that laboratory conditions for feeding experiments are different from those in natural settings. Differences in environmental conditions (i.e., water temperature, diet) and biological factors (i.e., age, size, type of tissues examined) may ultimately affect estimates of metabolic rates and Hg isotope turnover rates in PBFT (Tieszen et al., 1983; MacAvoy et al., 2006). We suggest that these factors should be taken into consideration when applying Hg isotope measurements in fish to trace sources and changes in MMHg under various environmental conditions and ecosystem types. Additional research that can link the internal behavior of Hg isotopes with more diverse environmental and biological parameters is expected to improve the applicability of Hg isotope studies of fish tissues to natural ecosystems.

References

Alex S, Savoie R. 1987. A Raman spectroscopic study of the complexation of the methylmercury(II) cation by amino acids. *Can J Chem* **65**: 491–496.

Bergquist BA, Blum JD. 2007. Mass-dependent and -independent fractionation of Hg isotopes by photoreduction in aquatic systems. *Science* **318**: 417–420.

Blank JM, Morrissette JM, Farwell CJ, Price M, Schallert RJ, et al. 2007. Temperature effects on metabolic rate of juvenile Pacific bluefin tuna *Thunnus orientalis*. *J Exp Biol* **210**: 4254–4261.

Block BA, Dewar H, Blackwell SB, Williams TD, Prince ED, et al. 2001. Migratory movements, depth, preferences, and thermal biology of Atlantic bluefin tuna. *Science* **293**: 1310–1314.

Blum JD, Bergquist BA. 2007. Reporting of variations in the natural isotopic composition of mercury. *Anal Bioanal Chem* **388**: 353–359.

Blum JD, Popp BN, Drazen JC, Choy CA, Johnson MW. 2013. Methylmercury production below the mixed layer in the North Pacific Ocean. *Nat Geosci* **6**: 879–884.

Bradley CJ, Madigan DJ, Block BA, Popp BN. 2014. Amino acid isotope incorporation and enrichment factors in Pacific bluefin tuna, *Thunnus orientalis*. *PLoS ONE* **9**: e85818 doi: 10.1371/journal.pone.0085818.

Buchheister A, Latour RJ. 2010. Turnover and fractionation of carbon and nitrogen stable isotopes in tissues of a migratory coastal predator, summer flounder (*Paralichthys dentatus*). *Can J Fish Aquat Sci* **67**: 445–461.

Caurant F, Navarro M, Amiard JC. 1996. Mercury in pilot whales: Possible limits to the detoxification process. *Sci Total Environ* **186**: 95–104.

Cerling T, Ayliffe L, Dearing M, Ehleringer J, Passey B, et al. 2007. Determining biological tissue turnover using stable isotopes: The reaction progress variable. *Oecologia* **151**: 175–189.

Choy CA, Popp BN, Kaneko JJ, Drazen JC. 2009. The influence of depth on mercury levels in pelagic fishes and their prey. *P Natl Acad Sci* **106**: 13865–13869.

Clark TD, Farwell CJ, Rodriguez LE, Brandt WT, Block BA. 2013. Heart rate responses to temperature in free-swimming Pacific bluefin tuna (*Thunnus orientalis*). *J Exp Biol* **216**: 3208–3214.

Coleman JA, Nogueira JI, Pancorbo OC, Batdorf CA, Block BA. 2015. Mercury in Pacific bluefin tuna (*Thunnus orientalis*): Bioaccumulation and trans-Pacific Ocean migration. *Can J Fish Aquat Sci* **72**: 1015–1023.

Corbeil M, Beauchamp AL, Alex S, Savoie R. 1986. Interaction of the methylmercury cation with glycine and alanine: A vibrational and X-ray diffraction study. *Can J Chemistry* **64**: 1876–1884.

Cossa DB, Averty B, Pirrone N. 2009. The origin of methylmercury in open Mediterranean waters. *Limnol Oceanogr* **54**: 837–844.

Cossa DB, Coquery M, Gobeil C, Martin JM. 1996. Mercury fluxes at the ocean margins, in Baeyens W, Ebinghaus R, Vasiliev O, eds., *Regional and Global Cycles of Mercury: Sources, Fluxes, and Mass Balances*. The Netherlands: Kluwer Academic.

Das K, Debacker V, Bouquegneau JM. 2000. Metallothionein in marine mammals. *Cell Mol Biol* **46**: 283–294.

Day RD, Roseneau DG, Berail S, Hobson KA, Donard OFX, et al. 2012. Mercury stable isotopes in seabird eggs reflect a gradient from terrestrial geogenic to oceanic mercury reservoirs. *Environ Sci Technol* **46**: 5327–5335.

Demers JD, Driscoll CT, Fahey TJ, Yavitt JB. 2007. Mercury cycling in litter and soil in different forest types in the Adirondack Region, New York, USA. *Ecol Appl* **17**: 1341–1351.

Drevnick PE, Lamborg CH, Horgan MJ. 2015. Increase in mercury in Pacific yellowfin tuna. *Environ Toxicol Chem* **9999**: 1–4.

Estess EE, Coffey DM, Shimose T, Seitz AC, Rodriguez L, et al. 2014. Bioenergetics of captive Pacific bluefin tuna (*Thunnus orientalis*). *Aquaculture* **434**: 137–144.

France RL. 1995. Critical examination of stable isotope analysis as a means for tracing carbon pathways in stream ecosystems. *Can J Fish Aquat Sci* **52**: 651–656.

Fry B. 2007. *Stable Isotope Ecology*. Baton Rouge, LA, USA: Springer Science and Business Media.

Gantner N, Hintelmann H, Zheng W, Muir DC. 2009. Variations in stable isotope fractionation of Hg in food webs of Arctic lakes. *Environ Sci Technol* **43**: 9148–9154.

Gehrke GE, Blum JD, Slotton DG, Greenfield BK. 2011. Mercury isotope link mercury in San Francisco Bay forage fish to surface sediment. *Environ Sci Technol* **45**: 1264–1270.

Giblin FJ, Massaro EJ. 1973. Pharmacodynamics of methyl mercury in the Rainbow Trout (*Salmo gairdneri*): Tissue uptake, distribution and excretion. *Toxicol Appl Pharmacol* **24**: 81–91.

Graham BS, Koch PL, Newsome SD, McMahon KW, Aurioles D. 2010. Using isoscapes to trace the movements and foraging behaviour of top predators in oceanic ecosystems, in West J, Bowen GJ, Dawson TE, Tu KP eds., *Isoscapes: Understanding Movement, Pattern and Process on Earth Through Isotope Mapping*. The Netherlands: Springer.

Hammerschmidt CR, Fitzgerald WF. 2006. Bioaccumulation and trophic transfer of methylmercury in Long Island Sound. *Arch Environ Contam Toxicol* **51**: 416–424.

Hannides CCS, Popp BN, Landry MR, Graham BS. 2009. Quantification of zooplankton trophic position in the North Pacific Subtropical Gyre using stable nitrogen isotopes. *Limnol Oceanogr* **54**: 50–61.

Hemre GI, Mommsen TP, Krogdahl A. 2002. Carbohydrate in fish nutrition: Effect on growth, glucose metabolism and hepatic enzymes. *Aquacult Nutr* **8**: 175–194.

Jardine TD, Kidd KA, Rasmussen JB. 2012. Aquatic and terrestrial organic matter in the diet of stream consumers: Implications for mercury bioaccumulation. *Ecol Appl* **22**: 843–855.

Jarvenpaa T, Tillander M, Miettinen JK. 1970. Methylmercury: Half-time of elimination in flounder, pike and eel. *Suom Kemistil B* **43**: 439–442.

Jiskra M, Wiederhold JG, Bourdon B, Kretzschmar R. 2012. Solution speciation controls mercury isotope fractionation of Hg(II) sorption to goethite. *Environ Sci Technol* **46**: 6654–6662.

Joiris CR, Holsbeek L, Moatemri NL. 1999. Total and methylmercury in sardines *Sardinella aurita* and *Sardina pilchardus* from Tunisia. *Mar Pollut Bull* **38**: 188–192.

Katz SL. 2002. Design of heterothermic muscle in fish. *J Exp Biol* **205**: 2251–2266.

Kitagawa T, Kimura S, Nakata H, Yamada H. 2004. Diving behavior of immature, feeding Pacific bluefin tuna (*Thunnus thynnus orientalis*) in relation to season and area: The East China Sea and the Kuroshio–Oyashio transition region. *Fish Oceanogr* **13**: 161–180.

Koster van Groos PG, Esser BK, Williams RW, Hunt JR. 2014. Isotope effect of mercury diffusion in air. *Environ Sci Technol* **48**: 227–233.

Krabbenhoft DP, Sunderland EM. 2013. Global change and mercury. *Science* **341**: 1457–1458.

Kraepiel AML, Keller K, Chin HB, Malcolm EG, Morel FMM. 2003. Sources and variations of mercury in tuna. *Environ Sci Technol* **37**: 5551–5558.

Kritee K, Barkay T, Blum JD. 2009. Mass dependent stable isotope fractionation of mercury during *mer* mediated microbial degradation of monomethylmercury. *Geochim Cosmochim Acta* **73**: 1285–1296.

Kwon SY, Blum JD, Carvan MJ, Basu N, Head JA, et al. 2012. Absence of fractionation of mercury isotopes during trophic transfer of methylmercury to freshwater fish in captivity. *Environ Sci Technol* **46**: 7527–7534.

Kwon SY, Blum JD, Chen CY, Meattey DE, Mason RP. 2014. Mercury isotope study of sources and exposure pathways of methylmercury in estuarine food webs in the Northeastern U.S. *Environ Sci Technol* **48**: 10089–10097.

Kwon SY, Blum JD, Chirby MA, Chesney EJ. 2013. Application of mercury isotopes for tracing trophic transfer and internal distribution of mercury in marine fish feeding experiments. *Environ Toxicol Chem* **23**: 2322–2330.

Kwon SY, Blum JD, Nadelhoffer KJ, Dvonch JT, Tsui MTK. 2015. Isotopic study of mercury sources and transfer between a freshwater lake and adjacent forest food web. *Sci Total Environ* **532**: 220–229.

Laffont L, Sonke JE, Maurice L, Monrroy SL, Chincheros J, et al. 2011. Hg speciation and stable isotope signature in human hair as a tracer for dietary and occupational exposure to mercury. *Environ Sci Technol* **45**: 9910–9916.

Lamborg CH, Von Damm KL, Fitzgerald WF, Hammerschmidt CR, Zierenberg R. 2006. Mercury and monomethylmercury in fluids from Sea Cliff submarine hydrothermal field, Gorda Ridge. *Geophys Res Lett* **33**: L17606.

Lares M L, Huerta-Diaz MA, Marinone SG, Valdez-Marquez M. 2012. Mercury and cadmium concentrations in farmed bluefin tuna (*Thunnus orientalis*) and the suitability of using the caudal peduncle muscle tissue as a monitoring tool. *J Food Protect* **75**: 725–730.

Lawson NM, Mason RP. 1998. Accumulation of mercury in estuarine food chains. *Biogeochem* **40**: 235–247.

Leaner JJ, Mason RP. 2002. Factors controlling the bioavailability of ingested methylmercury to Channel catfish and Atlantic sturgeon. *Environ Sci Technol* **36**: 5124–5129.

Li M, Sherman LS, Blum JD, Granjean P, Mikkelsen B, et al. 2014. Assessing sources of human methylmercury exposure using stable mercury isotopes. *Environ Sci Technol* **48**: 8800–8806.

MacAvoy S, Arneson L, Bassett E. 2006. Correlation of metabolism with tissue carbon and nitrogen turnover rate in small mammals. *Oecologia* **150**: 190–201.

Madigan DJ, Baumann Z, Carlisle AB, Hoen DK, Popp BN, et al. 2014. Reconstructing trans-oceanic migration patterns of Pacific bluefin tuna using a chemical tracer toolbox. *Ecology* **95**: 1674–1683.

Madigan DJ, Litvin SY, Popp BN, Carlisle AB, Farwell CJ, et al. 2012. Tissue turnover rates and isotopic trophic discrimination factors in the endothermic teleost, Pacific bluefin tuna (*Thunnus orientalis*). *PLoS ONE* **7**: 1–13.

Mason RP, Choi AL, Fitzgerald WF, Hammershmidt CR, Lamborg CH, et al. 2012. Mercury biogeochemical cycling in the ocean and policy implications. *Environ Res* **119**: 101–117.

McCloskey JT, Schultz IR, Newman MC. 1998. Estimating the oral bioavailability of methylmercury to channel catfish (*Ictalurus punctatus*). *Environ Sci Technol* **17**: 1524–1529.

Mergler D, Anderson HA, Chan LHM, Mahaffey KR, Murray M, et al. 2007. Methylmercury exposure and health effects in humans: A worldwide concern. *Ambio* **36**: 3–11.

Nakao M, Seoka M, Tsukamasa Y, Kawasaki K, Ando M. 2007. Possibility for decreasing of mercury content in bluefin tuna *Thunnus orientalis* by fish culture. *Fish Sci* **73**: 724–731.

Oliveira Ribeiro CA, Rouleau C, Pelletier E, Audet C, Tjalve H. 1999. Distribution kinetics of dietary methylmercury in the Arctic charr (*Salvelinus alpinus*). *Environ Sci Technol* **33**: 902–907.

Olson KR, Squibb KS, Cousins RJ. 1978. Tissue uptake, subcellular distribution, and metabolism of ^{14}CH$_3$HgCl and CH$_3$203HgCl by rainbow trout (*Salmo gairdneri*). *J Fish Res Board Can* **35**: 381–390.

Olson RJ, Duffy LM, Kuhnert PM, Galvan-Magana F, Bocanegra-Castillo N, et al. 2014. Decadal diet shift in yellowfin tuna *Thunnus albacares* suggests broad-scale food web changes in the eastern tropical Pacific Ocean. *Mar Ecol-Prog Ser* **497**: 157–178.

Perrot V, Bridou R, Pedrero Z, Guyoneaud R, Monperrus M, et al. 2015. Identical Hg isotope mass dependent fractionation signature during methylation by sulfate-reducing bacteria in sulfate and sulfate-free environment. *Environ Sci Technol* **49**: 1365–1373.

Perrot V, Pastukhov MV, Epov VN, Husted S, Donard OFX, et al. 2012. Higher mass-independent isotope fractionation of methylmercury in the pelagic food web of Lake Baikal (Russia). *Environ Sci Technol* **46**: 5902–5911.

Pethybridge HR, Young JW, Kuhnert PM, Farley JH. 2015. Using stable isotopes of albacore tuna and predictive models to characterize bioregions and examine ecological change in the SW Pacific Ocean. *Prog Oceanogr* **134**: 293–303.

Point D, Sonke JE, Day RD, Roseneau DG, Hobson KA, et al. 2011. Methylmercury photodegradation influenced by sea-ice cover in Arctic marine ecosystems. *Nat Geosci* **4**: 188–194.

Rabenstein DL, Isab AA, Reid RS. 1982. A proton nuclear magnetic resonance study of the binding of methylmercury in human erythrocytes. *Biochim Biophys Acta* **696**: 53–64.

Rodriguez-Gonzalez P, Epov VN, Bridou R, Tessier E, Guyoneud R, et al. 2009. Species-specific stable isotope fractionation of mercury during Hg(II) methylation by an anaerobic bacteria (*Desulfobulbus propionicus*) under dark conditions. *Environ Sci Technol* **43**: 9183–9188.

Schultz IR, Newman MC. 1997. Methyl mercury toxicokinetics in channel catfish (*Ictalurus punctatus*) and largemouth bass (*Micropterus salmoides*) after intravascular administration. *Environ Toxicol Chem* **16**: 990–996.

Senn DB, Chesney EJ, Blum JD, Bank MS, Maage A, et al. 2010. Stable isotope (N, C, Hg) study of methylmercury sources and trophic transfer in the Northern Gulf of Mexico. *Environ Sci Technol* **44**: 1630–1637.

Sherman LS, Blum JD. 2013. Mercury stable isotopes in sediment and largemouth bass from Florida lakes, USA. *Sci Total Environ* **448**: 163–175.

Sherman LS, Blum JD, Franzblau A, Basu N. 2013. New insight into biomarker of human mercury exposure using naturally occurring mercury stable isotopes. *Environ Sci Technol* **47**: 3403–3409.

Shimose T, Tanabe T, Hsu CC. 2009. Age determination and growth of Pacific bluefin tuna, *Thunnus orientalis*, off Japan and Taiwan. *Fish Res* **100**: 134–139.

Smith RS, Wiederhold JG, Kretzschmar R. 2015. Mercury isotope fractionation during precipitation of metacinnabar (ß-HgS) and montroydite (HgO). *Environ Sci Technol* **49**: 4325–4334.

Sunderland EM. 2007. Mercury exposure from domestic and imported estuarine and marine fish in the U.S. seafood market. *Environ Health Persp* **115**: 235–242.

Sunderland EM, Krabbenhoft DP, Moreau JW, Strode SA, Landing WM. 2009. Mercury sources, distribution, and bioavailability in the North Pacific Ocean: Insights from data and models. *Global Biogeochem Cy* **23**: 1–14.

Szczebak JT, Taylor DL. 2011. Ontogenetic patterns in bluefish (*Pomatomus saltatrix*) feeding ecology and the effect of mercury biomagnification. *Environ Toxicol Chem* **30**: 1447–1458.

Tieszen LL, Boutton TW, Tesdahl KG, Slade NA. 1983. Fractionation and turnover of stable carbon isotopes in animal tissues: Implications for δ^{13}C analysis of diet. *Oecologia* **57**: 32–37.

Tsui MTK, Blum JD, Finlay JC, Balogh SJ, Kwon SY, et al. 2013. Photodegradation of methylmercury in stream ecosystems. *Limnol Oceanogr* **58**: 13–22.

Tsui MTK, Blum JD, Finlay JC, Balogh SJ, Nollet YH, et al. 2014. Variation in terrestrial and aquatic sources of methylmercury in stream predators as revealed by stable mercury isotopes. *Environ Sci Technol* **48**: 10128–10135.

Tsui MTK, Blum JD, Kwon SY, Finlay JC, Balogh SJ, et al. 2012. Sources and transfers of methylmercury in adjacent river and forest food webs. *Environ Sci Technol* **46**: 10957–10964.

Whitlock RA, Walli A, Cermeño P, Rodriguez LE, Farwell C, et al. 2013. Quantifying energy intake in Pacific bluefin tuna (*Thunnus orientalis*) using the heat increment of feeding. *J Exp Biol* **216**: 4109–4123.

Weidel BC, Carpenter SR, Kitchell JF, Vander Zanden MJ. 2011. Rates and components of carbon turnover in fish muscle: Insights from bioenergetics models and a whole-lake ^{13}C addition. *Can J Fish Aquat Sci* **68**: 387–399.

Wiederhold JC, Cramer CJ, Daniel K, Infante I, Bourdon B, et al. 2010. Equilibrium mercury isotope fractionation between dissolved Hg(II) species and thiol-bound Hg. *Environ Sci Technol* **44**: 4191–4197.

York D. 1966. Least-squares fitting of a straight line. *Can J Phys* **44**: 1076–86.

Zheng W, Hintelmann H. 2009. Mercury isotope fractionation during photoreduction in natural water is controlled by its Hg/DOC ratio. *Geochim Cosmochim Acta* **73**: 6704–6715.

Contributions

- Contributed to conceptions and design: DJM, BNP
- Contributed to acquisition of data: SYK, DJM
- Contributed to analysis and interpretation of data: SYK, JDB, DJM
- Drafted and/or revised the article: SKY, JDB, DJM, BNP, BAB
- Approved the submitted version for publication: SYK, JDB, DJM, BNP, BAB

Mercury isotope dynamics in Pacific bluefin tuna

Competing interests

The authors declare no competing interests.

Data accessibility statement

All relevant data are included in this manuscript. Stable carbon and nitrogen isotope data of PBFT at additional time periods can be found in Madigan et al., 2012. Nitrogen isotope values of individual amino acids of PBFT can be found in Bradley et al., 2014.

Copyright